INDIANA GEOLOGICAL & WATER SURVEY
INDIANA UNIVERSITY

PETROFACIES AND RESIDUAL SATURATION IN A CAMBRIAN-ORDOVICIAN CARBONATE RESERVOIR FOR GEOLOGICAL SEQUESTRATION USING MERCURY POROSIMETRY

Medina, Cristian R.[1,2*], Mastalerz, M.[1], Rupp, J.[1]

[1]Indiana Geological & Water Survey, Indiana University, Bloomington, IN, USA; [2]Department of Earth and Atmospheric Sciences, Indiana University, Bloomington, IN, USA; *crmedina@indiana.edu

ABSTRACT

To better understand injection and post-injection flow processes and the entrapment of supercritical CO_2 during geological carbon sequestration in a carbonate reservoir, the pore systems were analyzed in sixty-six Cambrian-Ordovician carbonate samples from multiple states in the midwestern United States.

This work employed standard microphotography from thin sections, helium porosimetry for porosity and permeability, and mercury injection capillary pressure analysis, aiming to understand which elements of the pore system dominantly control the overall flow and CO_2 storage potential in the subsurface.

This work analyzes mercury injection capillary pressure data and proposes a petrophysical subdivision of the samples into four petrofacies, which is based on their values of porosity, permeability, and capillary entry pressure. This system aims to predict the portions of the studied carbonate sequence that are more likely to have a higher potential for injectivity and storage, and to better understand how porosity, permeability, capillary entry pressure, and pore size all play a role in ensuring both buoyant and capillary trapping mechanisms to secure the injected supercritical CO_2.

Results from this investigation suggest that in these Cambrian-Ordovician carbonate reservoirs, pore size inversely correlates with capillary entry pressure, and that permeability does not always hold a direct relationship with pore size, but rather with the overall interconnectivity of the complex pore system.

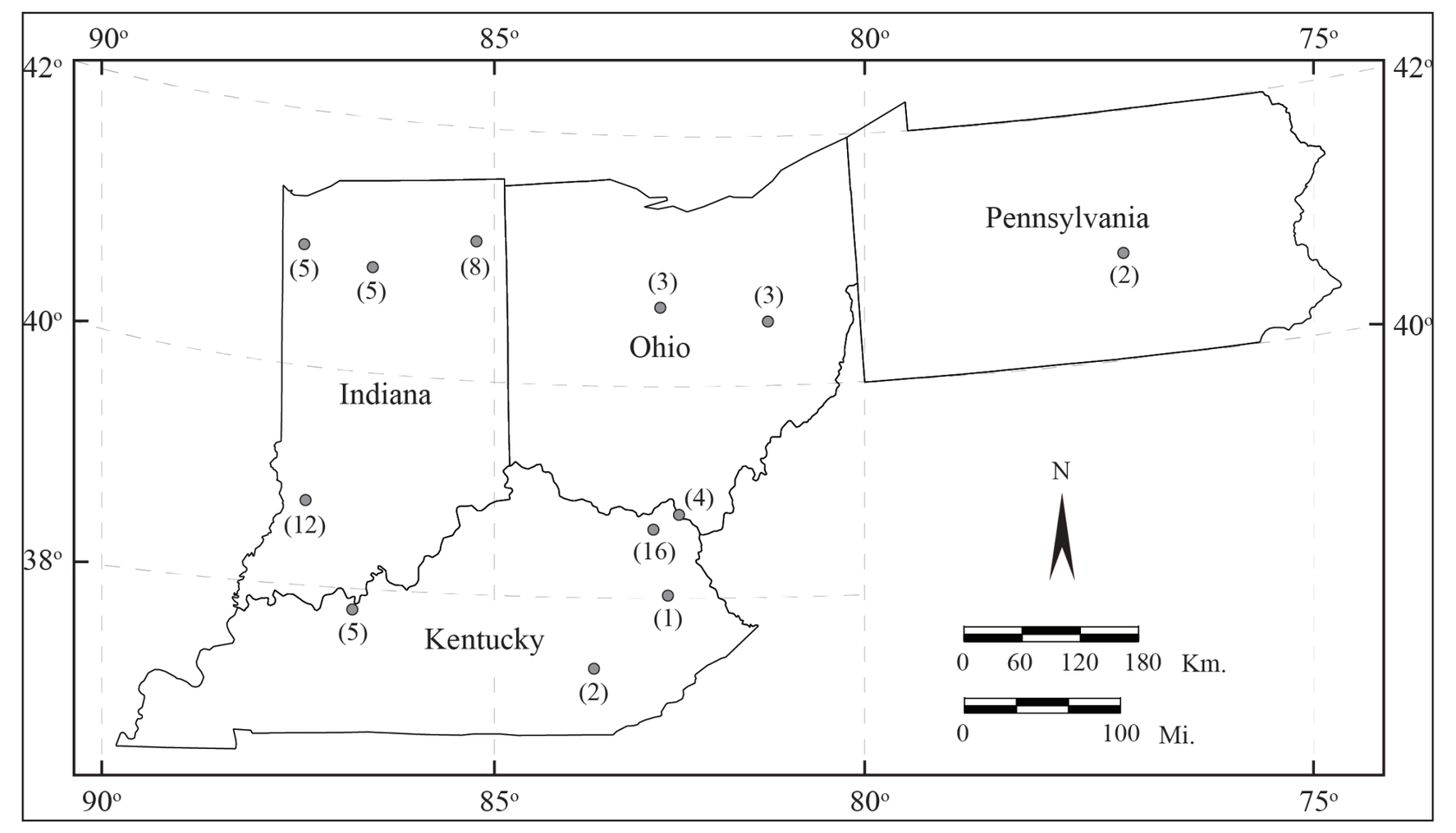

FIGURE 1. Map of the study area showing the 12 sample well locations with the number of samples per well in parentheses.

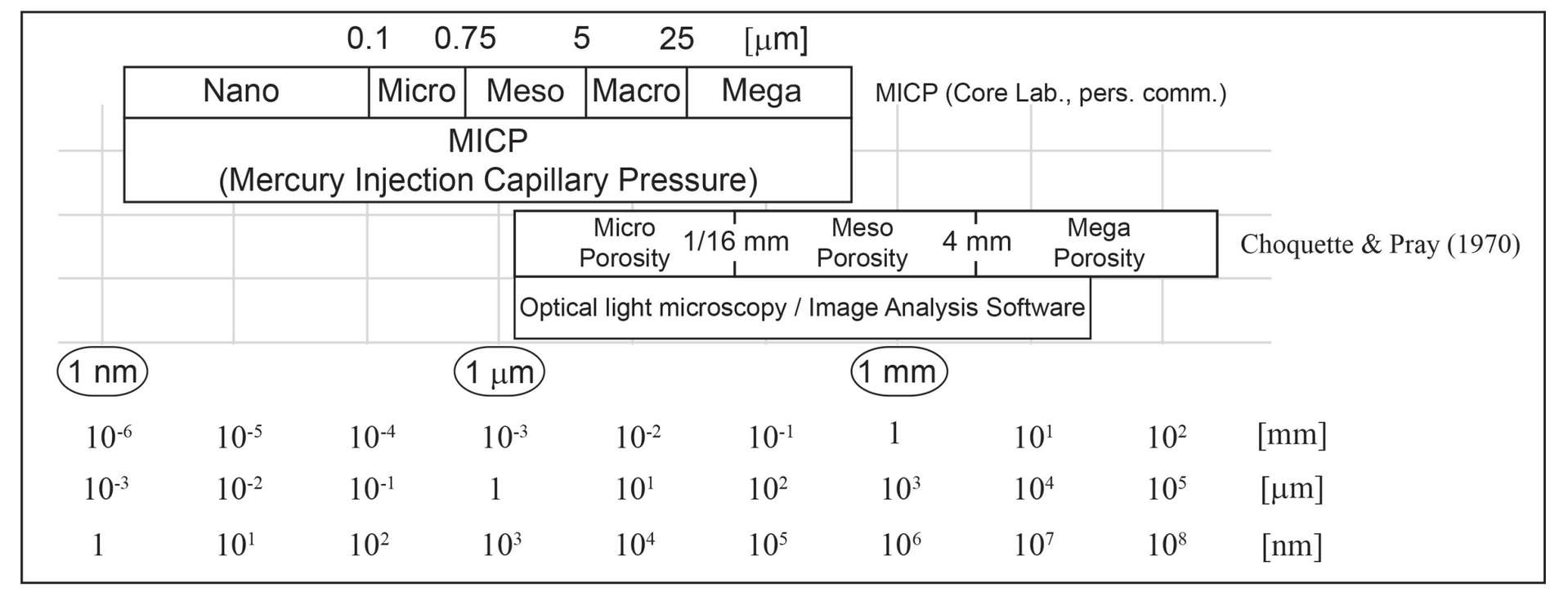

FIGURE 2: Ranges of pore size in MICP and in optical petrography/image analysis software.

1 WHAT AND WHY: INTRODUCTION AND PURPOSE

- Deep and widespread saline aquifers, such as those that occur in the Knox Supergroup in the midwestern region of the United States, offer suitable targets for CO_2 sequestration.
- The purpose of this paper is to evaluate the relationships between porosity and permeability and pore size distribution.
- This work aligns with one of the primary goals of the Midwest Regional Carbon Sequestration Partnership — to characterize and quantify the amount of resources (pore space) in saline aquifers for the geologic storage of carbon dioxide.

2 SAMPLES AND METHODOLOGY

- Studies of and comparison among techniques, such as image analysis from thin section, mercury injection capillary pressure tests (MICP) will help us understand the role and relative contribution to geologic storage of CO_2 provided by macro-, meso-, and microporosity (Fig. 2).

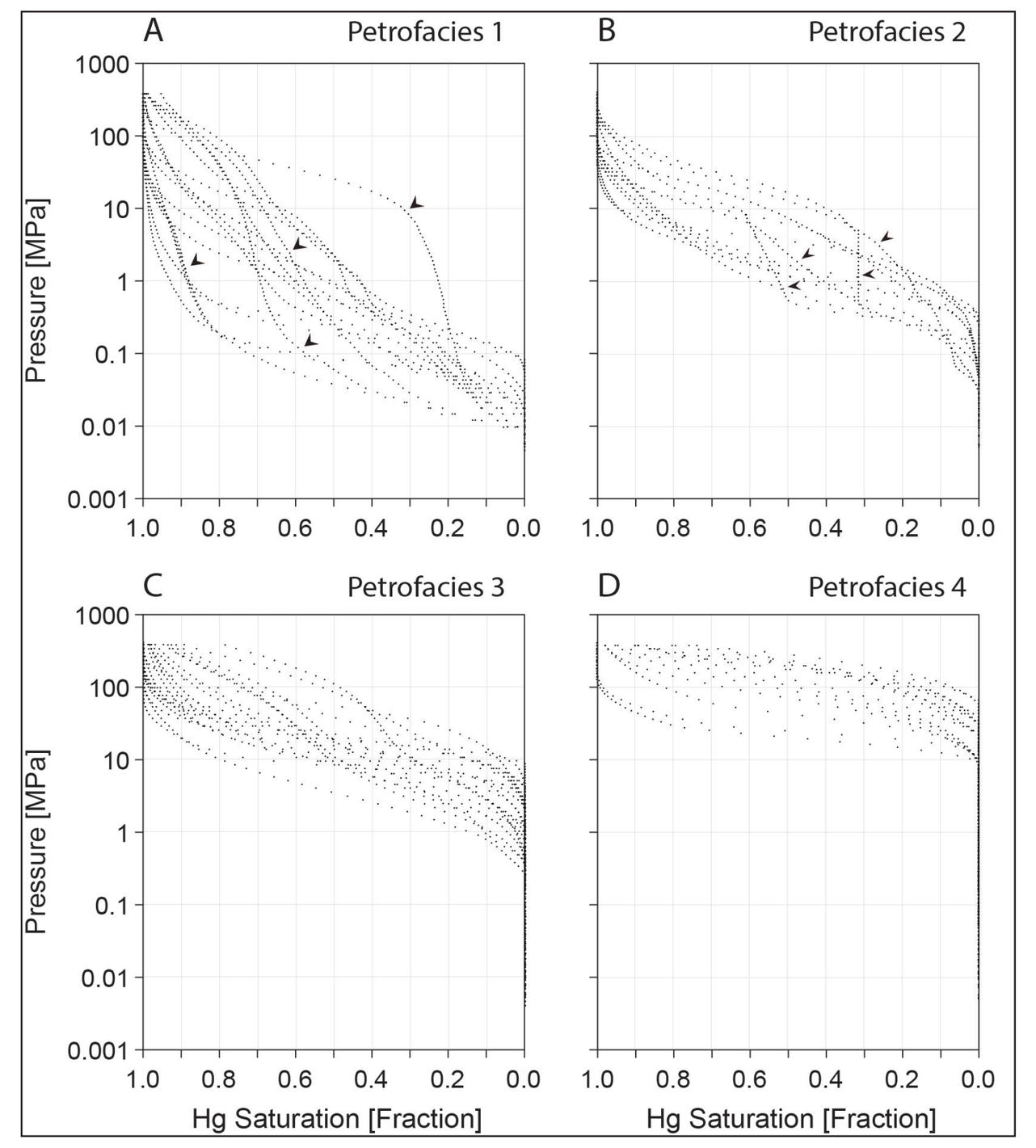

FIGURE 3: Capillary pressure of all samples studied, grouped by petrofacies number. In Petrofacies 1 and 2, the arrows indicate the anomalous trend of some samples.

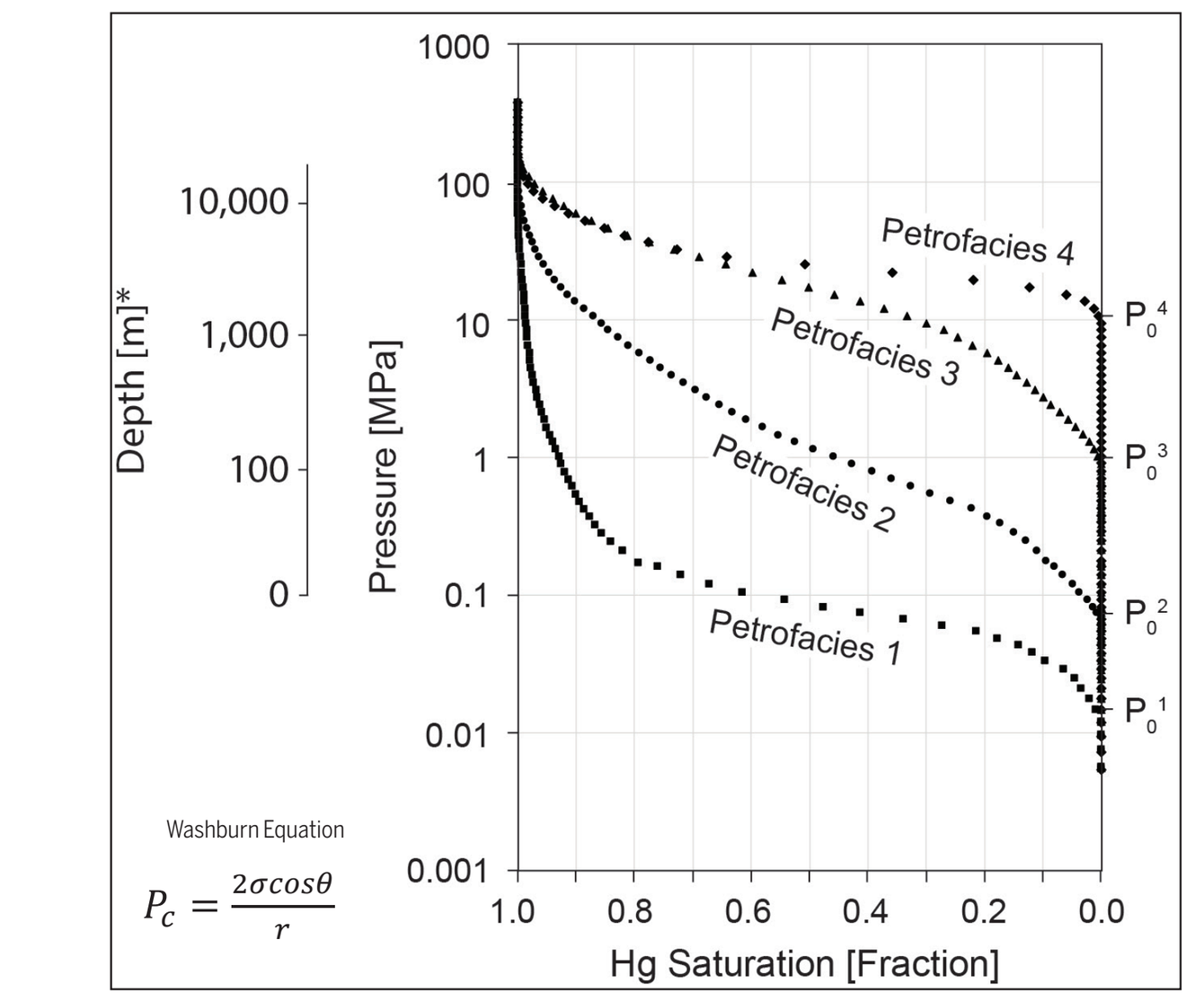

FIGURE 4: Samples used to exemplify heterogeneity exhibited in the same well (IGS #164778, Knox County, Indiana) from depth of: 1,345.39 m (Petrofacies 1, Po of 0.0138 MPa [2 psi]); 1,611.5 m (Petrofacies 2, Po of 0.0689 MPa [10 psi]); 1,611.26 m (Petrofacies 3, Po of 1.03 MPa [150 psi]); and 1,723.58 m (Petrofacies 4, Po of 10.34 MPa [1,500 psi]). *The left axis includes an auxiliary scale indicating reservoir pressures assuming a hydrostatic pressure gradient of 9.5 MPa/km (0.42 psi/ft).

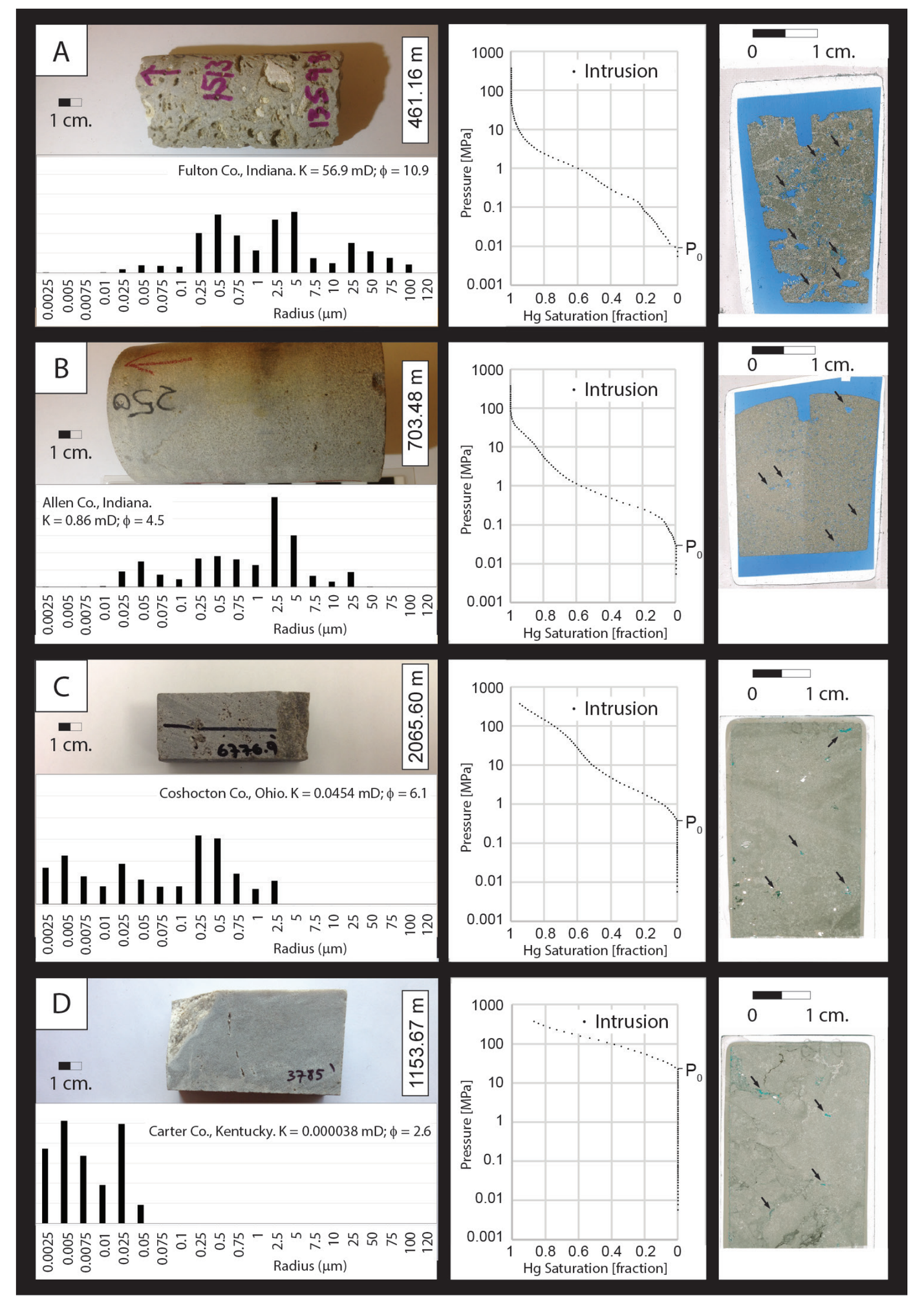

FIGURE 5. Representative samples of 4 petrofacies. Entry pressure is indicated in right side of capillary curve. A scanned photo of the thin section is included in right hand side, with arrows indicating some of the larger pores. (A) Petrofacies 1 (Low values of entry pressure, Po); (B) Petrofacies 2 (Low to intermediate values of Po); (C) Petrofacies 3 (intermediate to high values of Po); and (D) Petrofacies 4 (high values of Po). Each horizontal line in histograms represents 5% frequency of total Hg saturation.

3 RESULTS

- *Four groups with distinctive petrophysical properties were identified (Figs. 3-5).*
- *Each one of these groups also displays a particular pore-throat-size distribution (Figs. 5 and 10).*
- *There is a clear distinction between larger-pore-dominated samples (higher porosity and permeability) and smaller-pore-dominated sample (i.e. Fig. 5A vs. Fig. 5D).*
- *This method (MICP) results in a log-normal saturation curve (mercury injection curve, Figs. 3, 4, 5, and 11) that can be interpreted as analogous to a grain-size analysis in sedimentary rocks, where each injection pressure can be transformed to a pore size.*

Petrofacies	n	Entry Pressure						Permeability			Porosity	
		Ave. P_o [MPa]	GeoMean P_o [Mpa]	SD	Ave. P_{20} [Mpa]	Ave. P_{80} [Mpa]	GeoAve P [sqrt(P_{20}*P_{80})]	Arithmetic Average (k, mD)	Geometric Mean (k, mD)	SD	Average ϕ (%)	SD
1	17	0.0263	0.0185	0.0260	0.0913	22.6711	1.4385	74.4235	24.9483	121.9543	9.0059	6.2708
2	13	0.1702	0.1233	0.1336	0.7297	16.1969	3.4378	0.3730	0.1249	0.3886	4.5917	3.2595
3	22	2.1875	1.4088	2.1130	7.8588	85.7894	25.9653	0.0112	0.0040	0.0151	4.1609	2.2382
4	15	26.6027	21.0164	19.3108	72.3029	254.3242	135.6037	0.0002	0.0001	0.0003	3.5667	1.4064

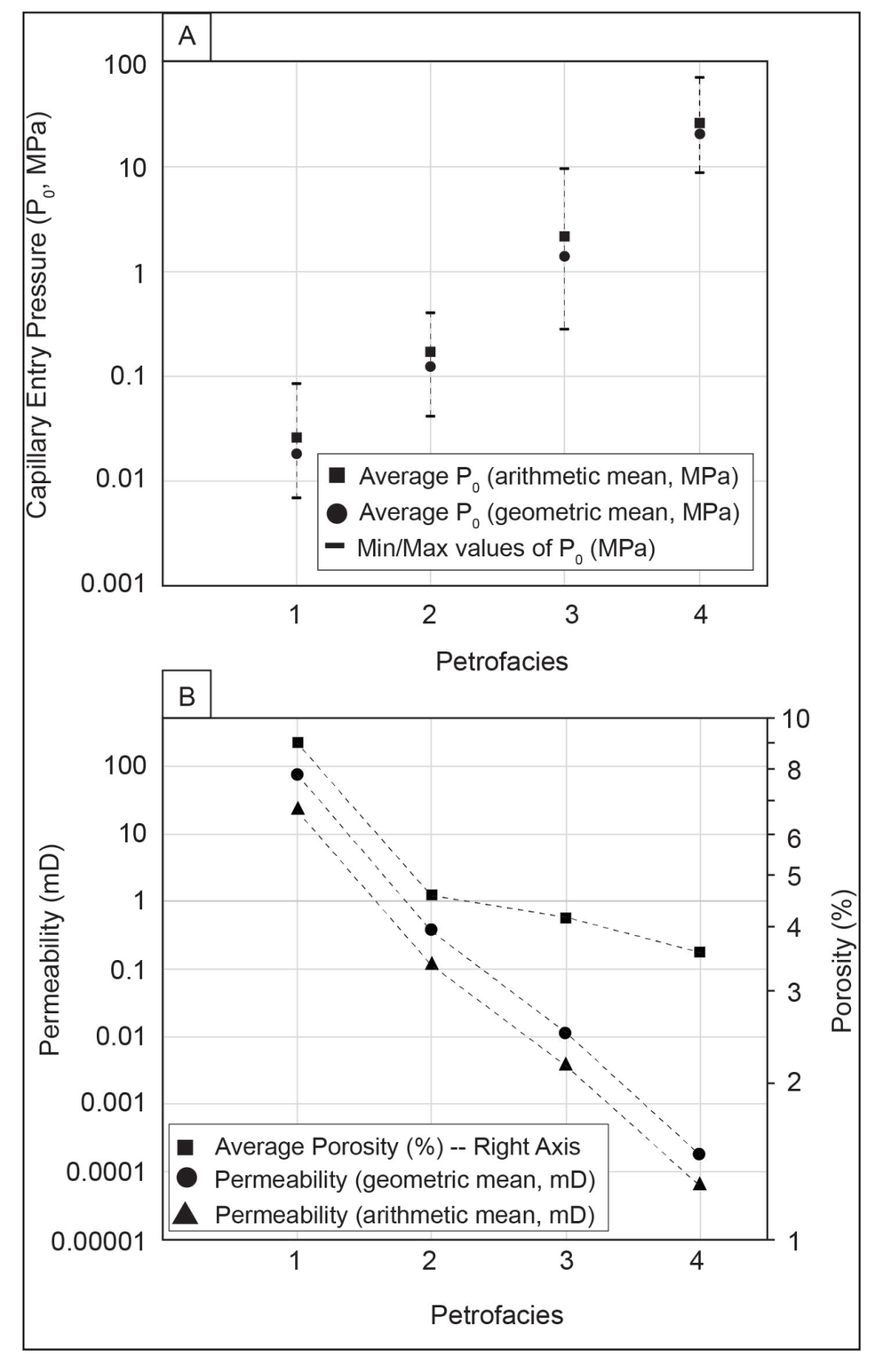

FIGURE 6. Arithmetic and geometric averages of A capillary entry pressure and B porosity and permeability from core analyses, sorted by petrofacies. In A, the maximum and minimum values of Po are indicated as whiskers.

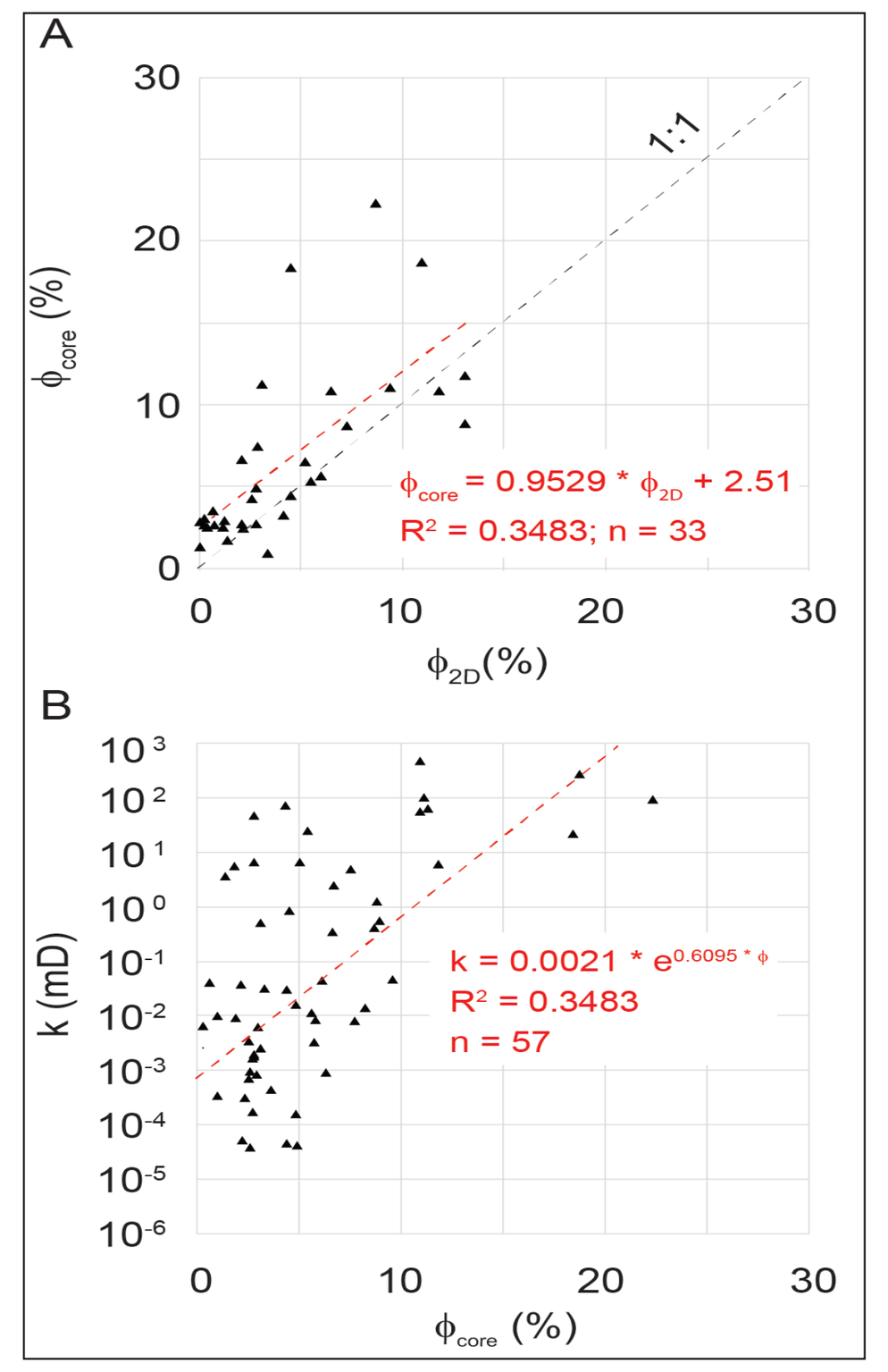

FIGURE 7. (A) Comparison of porosity from core analysis versus porosity from image analysis software (two-dimensional [2D] porosity) for 33 samples; (B) Permeability versus porosity obtained from core analysis of 57 samples.

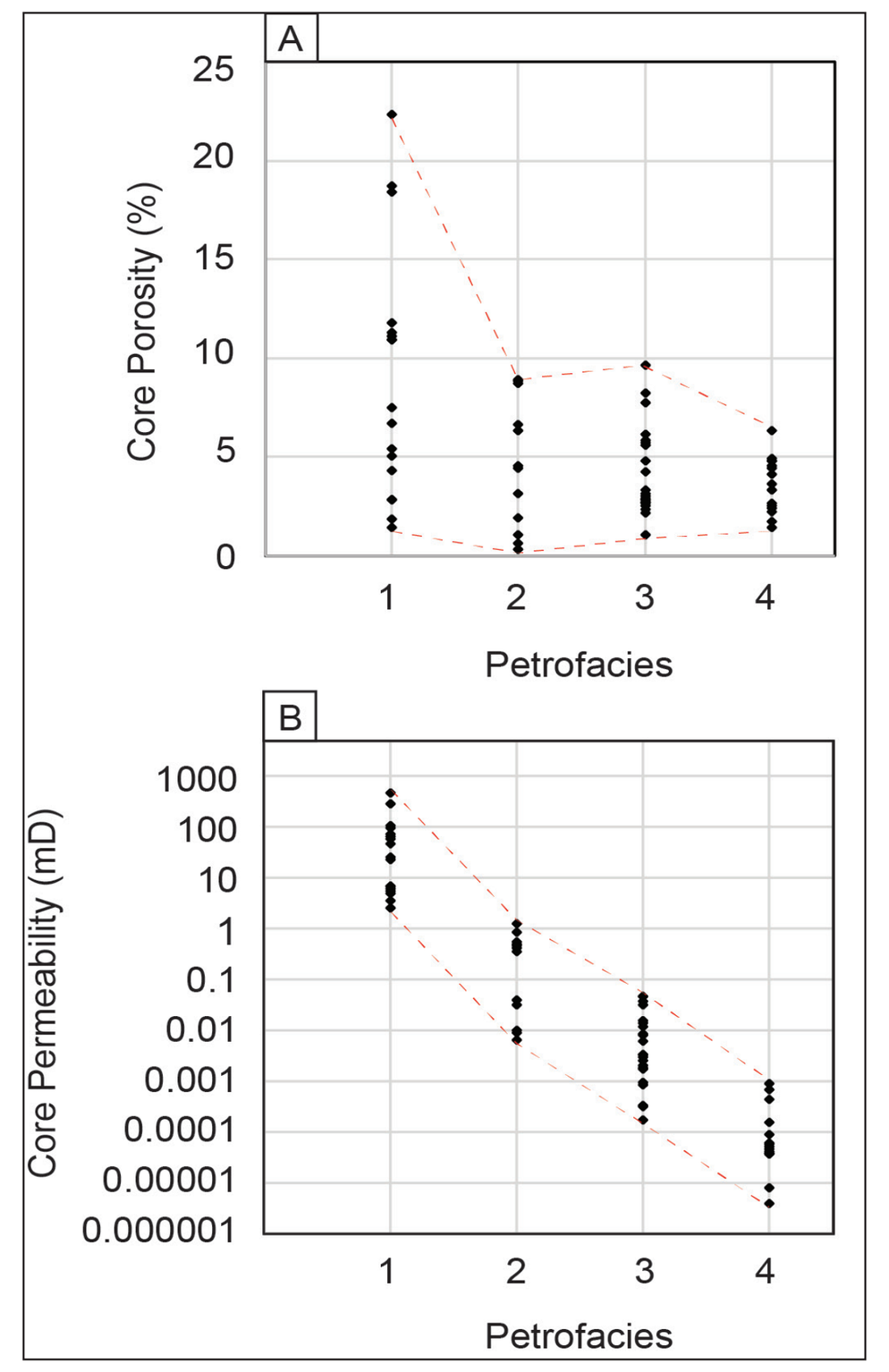

FIGURE 8. Porosity from core analysis (A) and permeability (B) from all samples in relationship to petrofacies number established from Po. Dotted lines indicate the envelope ranges for max and min values.

4 CONCLUSIONS

- Samples from the Knox Supergroup exhibit pore sizes that span several orders of magnitude. Pore-size distribution (Fig. 10) and pore connectivity (Fig. 11) seem to have a direct influence on permeability (Figs. 9-11).

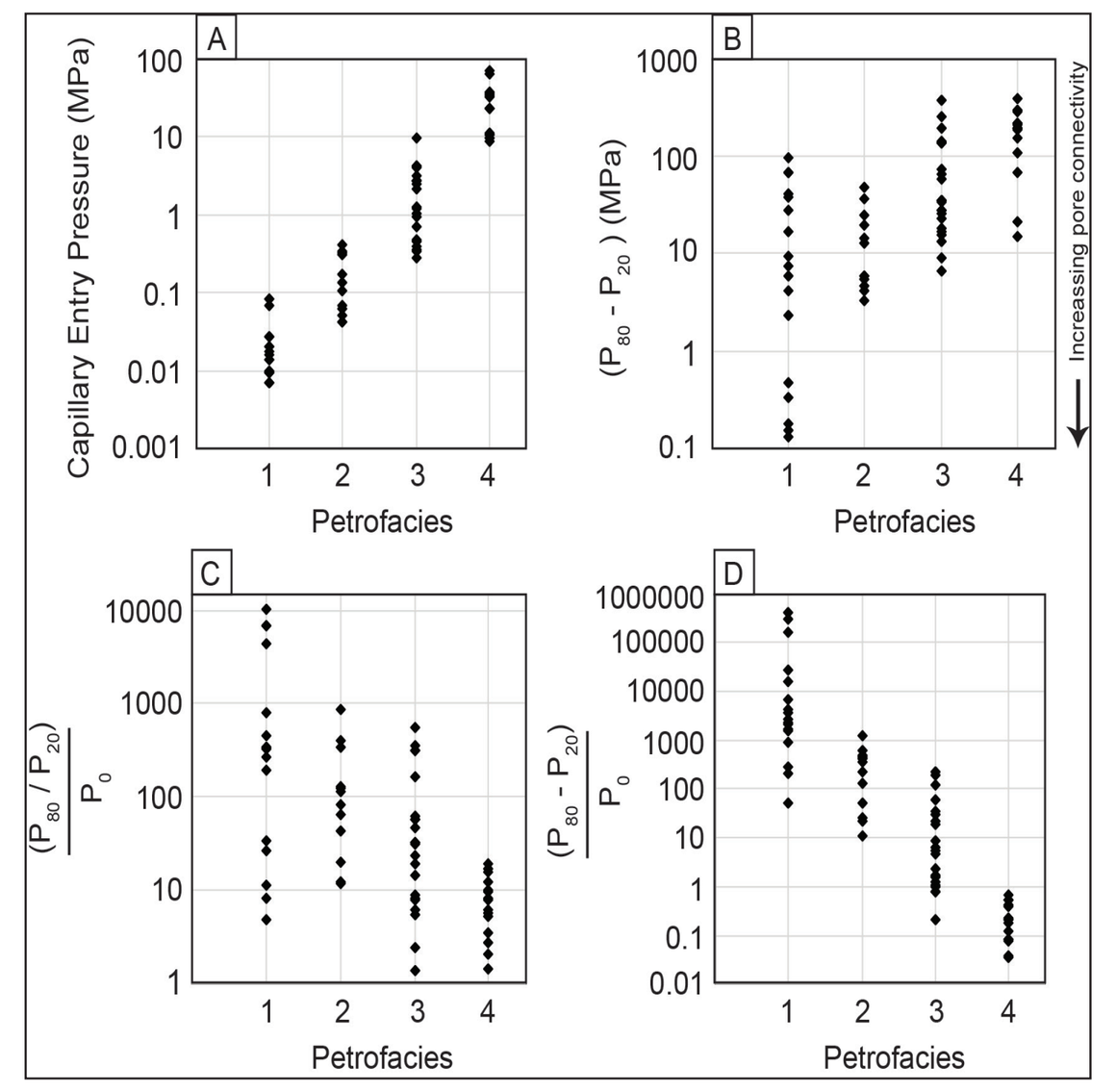

FIGURE 9. Several elements from capillary entry pressure curves, including Po, P_{20}, and P_{80}, and their relationship to petrofacies. (A) is illustrating Fig. 6A with all samples in this study. (B) is showing the net difference between P_{80} and P_{20}; (C) and (D) are normalizations of ratio and difference between P_{80} and P_{20}, respectively.

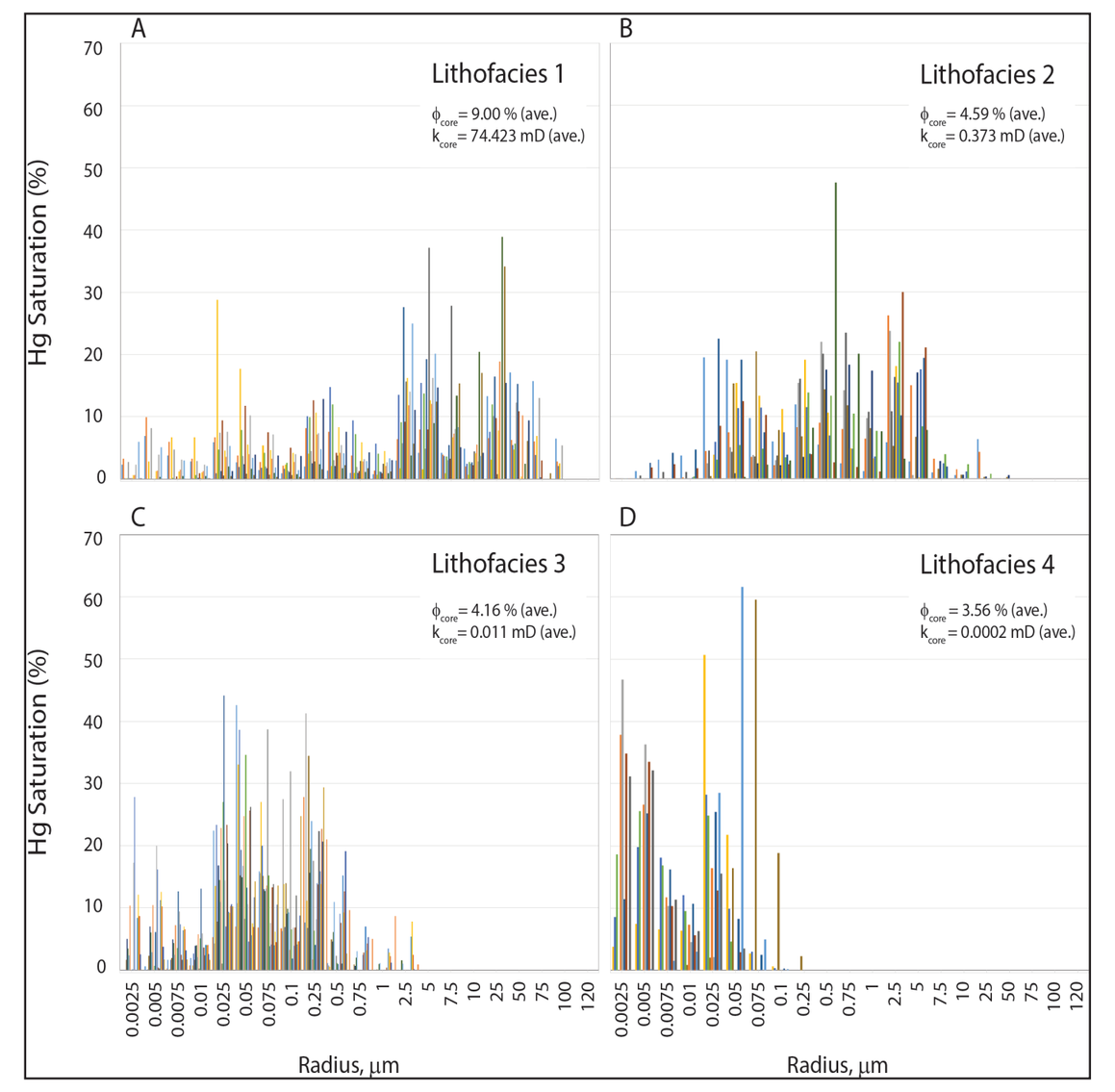

FIGURE 10. MICP-derived pore-throat size distribution from all samples. In this example, (A) Petrofacies 1 displays a bimodal distribution, with larger pores dominating flow; (B) Petrofacies 2 is dominated by intermediate pore throat size; (C) Petrofacies 3 is dominated by intermediate to low pore sizes; and (D) Petrofacies 4 has pore sizes smaller than 0.075 microns.

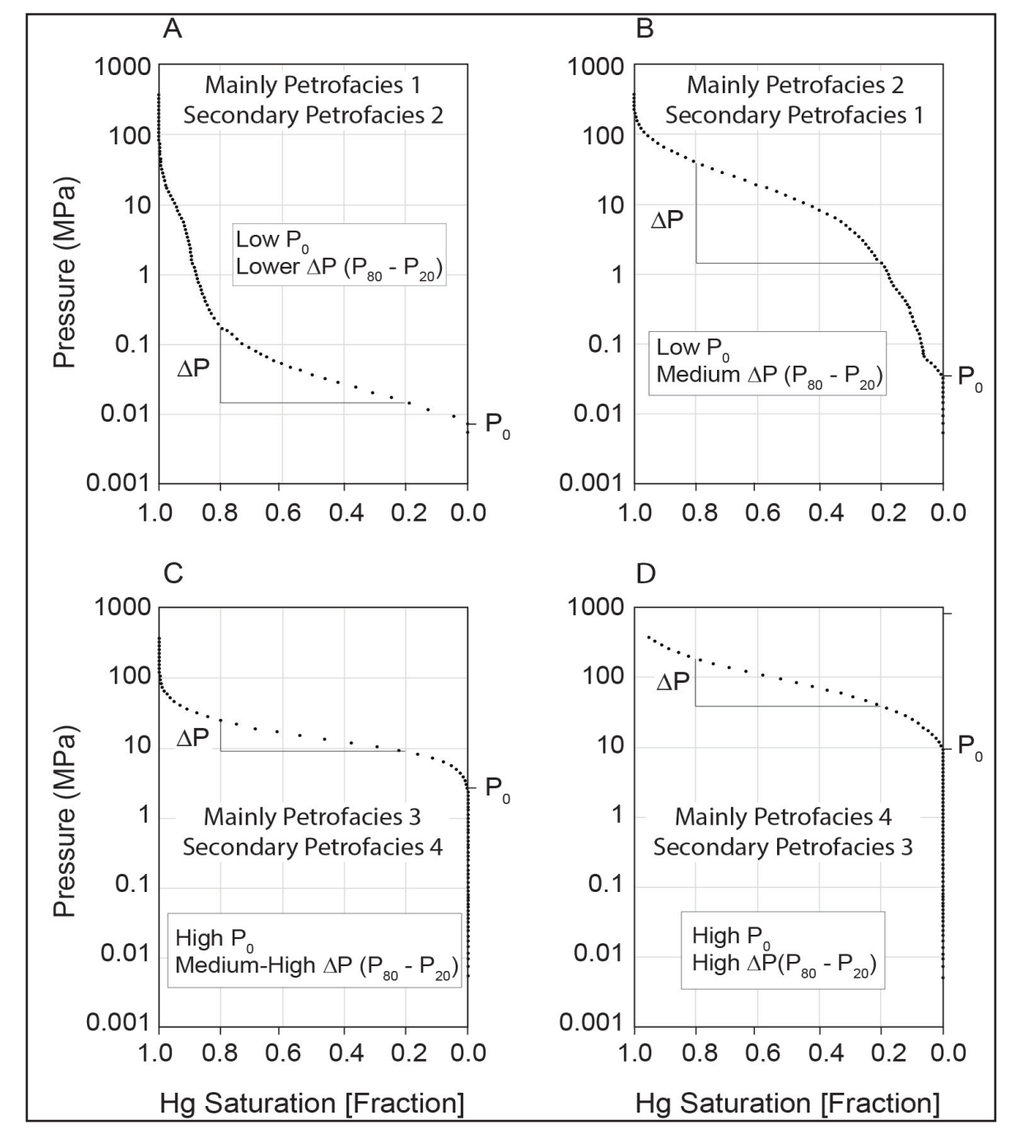

FIGURE 11. Further subdivision of the petrofacies using the position and shape of the curve. The samples used to exemplify this subdivision are as follows: (A) Well ID #133708 (Petrofacies 1 from Allen County, Indiana); (B) Well ID #135986 (Petrofacies 2 from Fulton County, Indiana); (C) Well ID #16051012430000 (Petrofacies 3 from Clay County, Kentucky); and (D) Well ID #16043001050000 (Petrofacies 4 from Carter County, Kentucky).

5 ACKNOWLEDGMENTS

This research was funded by the Department of Energy grant that supports research in carbon sequestration in the Midwest Regional Carbon Sequestration Partnership (MRCSP) region through the assistance of Battelle Institute.

MRCSP
MIDWEST REGIONAL CARBON SEQUESTRATION PARTNERSHIP